

A Probabilistic Approach Towards Robust Stability Optimization, with application to vibration control

L. Fenzi*, D. Pilbauer*,†, W. Michiels* and T. Vyhlídal†

*Department of Computer Science, KU Leuven

† Department of Instrumentation and Control Engineering, Faculty of Mechanical Engineering, and Czech Institute of Informatics, Robotics and Cybernetics, Czech Technical University in Prague

Summary. The main results of this paper concern the positioning and robust stability optimization of a mechanical system, to which a so-called delayed resonator is attached in order to absorb harmonic perturbations. Due to the inclusion of this active vibration suppression device, the overall closed-loop system is described by delay differential algebraic equations of retarded type. The stability optimization, thereby taking into account uncertainty on the mathematical model, is achieved by the design of static and dynamic controllers evaluated by minimizing an objective function, consisting of the mean of the spectral abscissa, the real part of the rightmost eigenvalue, with a variance penalty. The analysis and the dynamics of the system show the validity, efficacy and robustness of the novel approach, with respect to the results obtained by stability optimization without taking into account the uncertainty.

Introduction

The main goal of this paper is to validate the novel approach of [1] on a mechanical system with an active vibration suppression. The mechanical system, shown in Fig. 1, consists of two parts, a primary structure **P** which is affected by uncertainty and is excited by an external harmonic force f_e , and an absorber **A** attached to the primary structure with spring, damper and an actuator. The control objective of this paper is two-fold. Firstly, the external harmonic force is compensated by properly tuned parameters of the absorber. Secondly, the positioning of the system and robust stability of the induced equilibrium are ensured by a feedback controller, which acts on the primary structure with a force f_u , taking into account the uncertainty on the primary structure and the dynamics of the absorber.

The absorber is present in order to actively react on the external harmonic force with properly tuned feedback. The parameters of the feedback are tuned in order to turn the absorber to an ideal oscillator with a dominant couple of characteristic roots placed at the imaginary axis at the given input excitation frequency. As a consequence, the input harmonic force at the given frequency is suppressed entirely. The feedback in the absorber can accommodate position, velocity or acceleration measurements, depending on the particular application. In this paper, the main focus is on acceleration measurement as it is the most common in vibration control systems. Delay free methods were proposed in [2, 3]. However, due to the implementation aspects, these techniques lead to implementation difficulties, as shown in [4]. The active vibration control used in this paper utilizes delayed feedback, which goes back to [5–7]. Originally delayed feedback was based on a lumped delay which has been shown as undesirable when the feedback is taken from acceleration, where the delay is in the presence of derivative feedback. Therefore, the closed loop dynamics becomes a neutral time delay system [8]. This class of system may have an undesirable high sensitivity to small delay perturbations [9, 10]. Due to this, we utilize recently developed delayed feedback with distributed time delay, proposed in [11]. It has been shown in [11] that acceleration feedback with distributed time delay has advantages from both the theoretical and practical point of view, as it provides retarded dynamics and it acts like as a moving average filter on the measurements. On the other hand, the delayed feedback always introduces infinitely many characteristic roots and the system is then described in terms of delay differential equations.

In order to position the primary structure and optimize the response time in spite of the uncertainty on the primary mass, a feedback controller is used, see Fig. 1. The stability optimization methods permit to design an off-line state feedback controller which can be either static or dynamic. The majority of these approaches are interested in minimizing the spectral

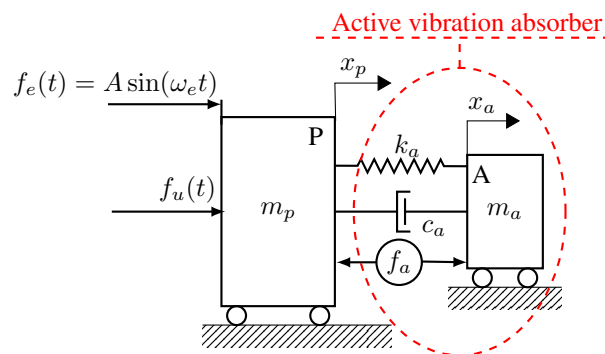


Figure 1: Mechanical system with active vibration absorber.

abscissa, which is the real part of the rightmost eigenvalue [12–15], assuming that accurate parameter measurements are available. However these methods may lead to a very sensitive solution, where a small variation of the parameter of the system may cause deteriorated performance or even destabilize the system. More robust solutions are traditionally designed by bifurcation analysis or within the robust control or pseudo-spectral frameworks, see [16] and the reference therein. The former restrict to a small number of (control and uncertain) parameters. The latter is based on a worst-case analysis which exploits only upper bounds. In order to take into account the uncertainty on the primary structure and obtain robustly stable dynamics, we utilize the novel approach [1], grounded in a probabilistic setting. This stability optimization approach exploits the structure of the uncertainty, described by continuous random vector $\boldsymbol{\omega}$ with a given statistical distribution $p_{\boldsymbol{\omega}}(\boldsymbol{\omega})$, minimizing the mean of the spectral abscissa with a variance penalty. As a result, we show that these latter controllers provide increased robust stability properties than the controllers obtained with the deterministic stability optimization method [12]. The validation of the novel approach [1] is, hence, accomplished by the analysis of the step responses for different nominal value of the primary mass m_p .

The structure of the paper is as follows. In the following section the main features of the method from [1] are reviewed. Afterwards, the efficacy and usability of the approach is presented on the active vibration suppression system with two control objectives. At the end, we close the paper by outlining the main results and drawing our conclusions.

Robust stability optimization in a probabilistic setting

In this section we review the novel method proposed in [1]. First of all, the generic system description and the definition of the optimization problem are presented. The optimization problem is addressed theoretically, showing the existence of the objective function and its gradient. Then, a numerical method to evaluate the objective function and its gradient is proposed. Finally, at the end of the section, the main features of the optimization problem are explained and a sketch of the overall algorithm is presented.

For the sake of conciseness, theoretical results from this section are stated without proof, which can be found in the accompanying paper [1].

System description and definition of the optimization problem

The presented framework supports a system description by means of linear delay differential algebraic equations of retarded type, which arise from the feedback interconnection of a delay system of retarded type and a controller, where either the plant or the controller is strictly proper:

$$E\dot{x}(t) = \sum_{i=0}^h A_i(\boldsymbol{\omega}, \mathbf{K})x(t - \tau_i(\boldsymbol{\omega})), \quad (1)$$

where

- $x(t) \in \mathbb{R}^n$ represents the state at time $t \geq \max_{\boldsymbol{\omega} \in \mathbb{S}} \{-\tau_i(\boldsymbol{\omega}) : i = 1, \dots, h\}$;
- $\boldsymbol{\omega} \in \mathbb{S} \subset \mathbb{R}^D$ are the possible values of the uncertain parameters, which are described by the continuous real random vector $\boldsymbol{\omega}$ with support $\mathbb{S} = [0, 1]^D$ and probability density function

$$p_{\boldsymbol{\omega}} : \mathbb{S} \rightarrow \mathbb{R}_{\geq 0}, \quad \boldsymbol{\omega} \mapsto p_{\boldsymbol{\omega}}(\boldsymbol{\omega}),$$

that we assume to be smooth;

- $\mathbf{K} \in \mathbb{R}^k$ parametrizes the controller;
- E is a real matrix and it is allowed to be singular;
- For every $i \in \{0, \dots, h\}$ $A_i : \mathbb{S} \times \mathbb{R}^k \rightarrow \mathbb{R}^{n \times n}$, $(\boldsymbol{\omega}, \mathbf{K}) \mapsto A_i(\boldsymbol{\omega}, \mathbf{K})$, and $\tau_i : \mathbb{S} \rightarrow \mathbb{R}_{\geq 0}$, $\boldsymbol{\omega} \mapsto \tau_i(\boldsymbol{\omega})$ are functions which we assume to be smooth.

For given $(\boldsymbol{\omega}, \mathbf{K}) \in \mathbb{S} \times \mathbb{R}^k$, the stability properties of the system (1) are determined by the spectrum of its characteristic matrix

$$\Lambda(\lambda; \boldsymbol{\omega}, \mathbf{K}) = \lambda E - \sum_{i=0}^h A_i(\boldsymbol{\omega}, \mathbf{K})e^{-\lambda\tau_i(\boldsymbol{\omega})}. \quad (2)$$

Since we are dealing with delay differential algebraic equation of retarded type, the characteristic matrix $\Lambda(\lambda; \boldsymbol{\omega}, \mathbf{K})$ admits finitely many eigenvalues in any right half-plane. Consequently, the trivial solution of (1) is asymptotically stable if and only if the spectral abscissa $\alpha(\boldsymbol{\omega}, \mathbf{K})$ is strictly negative, where the latter is defined as the real part of the rightmost eigenvalue

$$\alpha(\boldsymbol{\omega}, \mathbf{K}) = \max_{\lambda \in \mathbb{C}} \{\Re(\lambda) : \det(\Lambda(\lambda; \boldsymbol{\omega}, \mathbf{K})) = 0\}. \quad (3)$$

In order to take into account uncertainty in the stability optimization problem, our goal is to minimize a specific linear combination of the mean and the variance of the spectral abscissa, in formula:

$$\min_{\mathbf{K} \in \mathbb{R}^k} f_{\text{obj}}(\mathbf{K}), \text{ with } f_{\text{obj}}(\mathbf{K}) = \mathbb{E}(\alpha(\boldsymbol{\omega}, \mathbf{K})) + c \cdot \text{Var}(\alpha(\boldsymbol{\omega}, \mathbf{K})), \quad (4)$$

where $c \in \mathbb{R}_{\geq 0}$ is a given trade off parameter, and $\mathbb{E}(\cdot)$ and $\text{Var}(\cdot)$ indicate the mean and the variance, respectively.

In order to develop the present approach, we need the following assumption which is not restrictive from the application point of view: for fixed \mathbf{K} in \mathbb{R}^k the rightmost eigenvalue is simple for almost all $\omega \in \mathbb{S}$, and for fixed $\omega \in \mathbb{S}$ the rightmost eigenvalue is simple for almost all $\mathbf{K} \in \mathbb{R}^k$.

Existence of the objective function and its gradient

Objective function (4) is a linear combination of two integrals, namely $\mathbb{E}(\alpha(\boldsymbol{\omega}, \mathbf{K}))$ and $\text{Var}(\alpha(\boldsymbol{\omega}, \mathbf{K}))$, which depend on the behavior of the spectral abscissa varying $\omega \in \mathbb{S}$.

The spectral abscissa of the retarded system (1) is a continuous function [10]. Moreover, by the made assumptions, it is smooth for almost all $\omega \in \mathbb{S}$, however in a set of measure zero there might be more than one rightmost eigenvalue counted with multiplicity. If there are more than one rightmost eigenvalue we can distinguish two cases: the rightmost eigenvalues are (semi)-simple or there is at least one eigenvalue non-semisimple. In the first case the spectral abscissa still presents a Lipschitz continuous behavior, but its derivative has bounded discontinuities. In the latter case, the spectral abscissa is typically not even Lipschitz continuous and its derivative may present unbounded discontinuities.

The behavior of the spectral abscissa guarantees that objective function (4) exists for all $\mathbf{K} \in \mathbb{R}^k$ (Proposition 1 in [1]). Furthermore, if the gradient of the spectral abscissa w.r.t. the control parameters \mathbf{K} is integrable over \mathbb{S} , then the gradient of objective function (4) exists and can be expressed by the following formula (Proposition 3 in [1]):

$$\nabla_{\mathbf{K}} f_{\text{obj}}(\mathbf{K}) = [1 - 2c\mathbb{E}(\alpha(\boldsymbol{\omega}, \mathbf{K}))]\mathbb{E}(\nabla_{\mathbf{K}}\alpha(\boldsymbol{\omega}, \mathbf{K})) + 2c\mathbb{E}(\alpha(\boldsymbol{\omega}, \mathbf{K})\nabla_{\mathbf{K}}\alpha(\boldsymbol{\omega}, \mathbf{K})). \quad (5)$$

Under global Lipschitz condition on the spectral abscissa, its gradient is integrable over the uncertain domain \mathbb{S} (Theorem 5 in [1]), and hence the gradient of the objective function exists. Even though we are not able to prove that $\nabla_{\mathbf{K}} f_{\text{obj}}(\mathbf{K})$ exists for all $\mathbf{K} \in \mathbb{R}^k$, we have strong indication that this property holds (Example 1 in [1]).

Approximation of the objective function and its gradient

The computation of objective function (4) is based on approximating integrals:

$$\begin{aligned} \mathbb{E}(\alpha(\boldsymbol{\omega}, \mathbf{K})) &= \int_{\mathbb{S}} \alpha(\omega, \mathbf{K}) p_{\omega}(\omega) d\omega, \\ \text{Var}(\alpha(\boldsymbol{\omega}, \mathbf{K})) &= \mathbb{E}(\alpha(\boldsymbol{\omega}, \mathbf{K})^2) - \mathbb{E}(\alpha(\boldsymbol{\omega}, \mathbf{K}))^2. \end{aligned} \quad (6)$$

Since the integrands of (6) show a continuous non-differentiable behavior, the numerical integration is accomplished by Quasi-Monte Carlo methods [17–19]. Indeed, the Quasi-Monte Carlo integration is almost as accurate as the Monte Carlo method, but it improves the convergence rate of standard Monte Carlo method if the integrand is smooth [19].

As suggested by [18], we construct a set $\Xi = \{\omega^i\}_{i=1}^M$ of M quasi-random points uniformly distributed in the D -dimensional unit cube using the Halton sequences. For every $\omega^i \in \Xi$, evaluating the spectral abscissa $\alpha(\omega^i, \mathbf{K})$ of (1), we can approximate integrals (6), *i.e.* the mean of $\alpha(\boldsymbol{\omega}, \mathbf{K})$, using the following formula:

$$\mathbb{E}(\alpha(\boldsymbol{\omega}, \mathbf{K})) \approx \frac{1}{M} \sum_{i=1}^M \alpha(\omega^i, \mathbf{K}) p_{\omega}(\omega^i), \quad (7)$$

and a similar formula can be applied to evaluate the Variance.

The approximation of the spectral abscissa $\alpha(\omega^i, \mathbf{K})$, for the deterministic systems (1), *i.e.* for a fixed realization $\omega \in \Xi$, is accomplished by the Infinitesimal Generator Approach [12, 20, 21].

Moreover, whenever the rightmost eigenvalue $\lambda(\omega, \mathbf{K})$ is simple we can explicitly express its partial derivative w.r.t. the control parameters in terms of its right and left eigenvectors ($v, u \in \mathbb{C}^n$ respectively) and of its characteristic matrix $\Lambda(\lambda; \omega, \mathbf{K})$ as stated in Lemma 2.7 in [22]. This result provides us an explicit formula for the partial derivative of the spectral abscissa w.r.t. K_j for $j = 1, \dots, k$:

$$\frac{\partial \alpha(\omega, \mathbf{K})}{\partial K_j} = \Re \left(\frac{-u(\omega, \mathbf{K})^* \frac{\partial \Lambda(\lambda; \omega, \mathbf{K})}{\partial K_j} v(\omega, \mathbf{K})}{u(\omega, \mathbf{K})^* \frac{\partial \Lambda(\lambda; \omega, \mathbf{K})}{\partial \lambda} v(\omega, \mathbf{K})} \right), \quad a.e. (\omega, \mathbf{K}) \in \mathbb{S} \times \mathbb{R}^k. \quad (8)$$

From a computational point of view, we compute the spectral abscissa at only a finite number of points where we can expect $\alpha(\omega, \mathbf{K})$ to be differentiable. Hence, with the realizations $\frac{\partial \alpha(\omega, \mathbf{K})}{\partial K_j}$ for $\omega \in \Xi$, we can approximate the gradient of the objective function (5) through an analogous formula of (7).

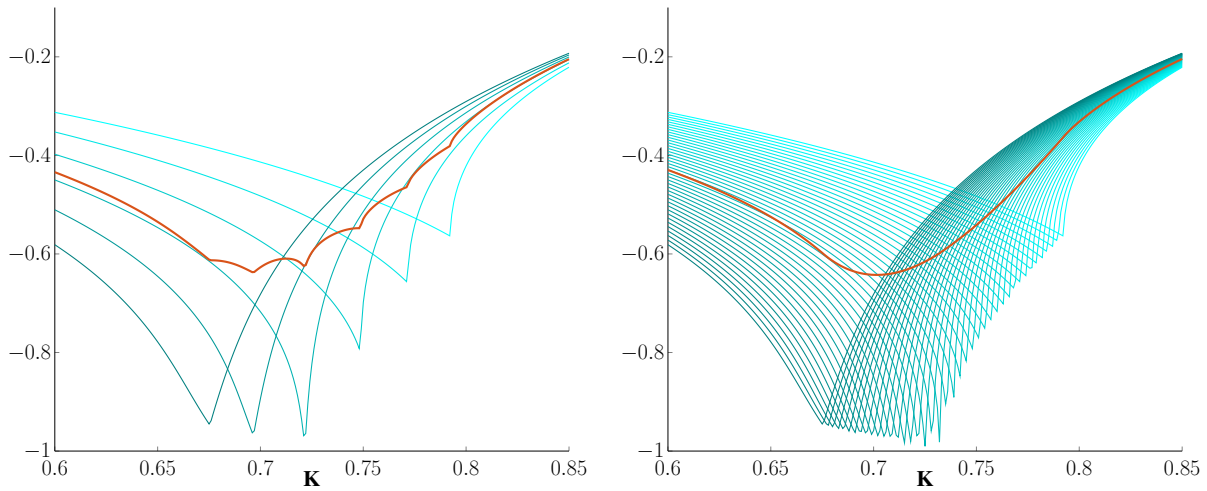


Figure 2: Spectral abscissa functions (blue line) and their mean (red line) for system (23) in [1]. On the left pane the mean is obtained averaging 6 abscissa functions, while on the right pane the mean is calculated on 201 spectral abscissa functions.

Solving the optimization problem

By the made assumptions, we are theoretically dealing with an objective function which is everywhere differentiable under mild assumptions, due to the smoothing effect of the integration. We obtain, hence, a smoother optimization problem than the deterministic spectral abscissa optimization problem (right pane of Fig. 2). However the numerical integration (7) leads to a non-smooth objective function, which is more regular than the spectral abscissa but presents further local minima, as stressed by the left pane of Fig. 2. This is because by the discretization of the integral, its smoothing effect is lost (red line in the left pane of Fig. 2).

The properties of the optimization problem requires optimization software which can deal with non-convex and non-smooth unconstrained minimization. The optimization is accomplished by MATLAB code HANSO (Hybrid Algorithm for Non-Smooth Optimization) [13], requiring the approximated objective function and its gradient.

Since an accurate computation of f_{obj} and $\nabla_{\mathbf{K}} f_{\text{obj}}$ is computationally demanding, we focus on a deterministic description of the random parameters $\boldsymbol{\omega}$, fixing a set $\Xi_{\text{opt}} = \{\omega^i\}_{i=1}^{M_{\text{opt}}}$ of M_{opt} realizations in \mathbb{S} . Hence, the objective function and its gradient are always approximated on Ξ_{opt} , in such a way that the fluctuations of the realizations of $\boldsymbol{\omega}$ will not effect the accuracy of the optimization solver.

In order to compute optimal gain values \mathbf{K} , the HANSO algorithm is initialized by default on 15 random starting vectors. To check local optimality of the returned solution, it is convenient to compute the objective function and its gradient on a refined grid Ξ_{post} , with $M_{\text{opt}} \ll M_{\text{post}}$. If the norm of the latter gradient is approximately zero, then the accuracy M_{opt} , used to compute the optimal gain value, is enough to obtain reliable solutions; otherwise we refine the sample Ξ_{opt} and we run HANSO again, initialized with the optimal gain value \mathbf{K} obtained with the previous rough grid.

To give an overview of the method, we provide a sketch of the overall algorithm, which is publicly available [23].

Algorithm 1

1. Construct a set of M_{opt} realizations of $\boldsymbol{\omega}$, i.e. Ξ_{opt} , using the Halton sequence.
 2. Via HANSO, find the optimal gain value for (1), giving as inputs the approximations of the objective function and its gradient on Ξ_{opt} .
 3. Likewise step 1, construct a set of M_{post} realizations of $\boldsymbol{\omega}$, i.e. Ξ_{post} .
 4. Approximate f_{obj} and $\nabla_{\mathbf{K}} f_{\text{obj}}$ on Ξ_{post} .
- if $\|\nabla_{\mathbf{K}} f_{\text{obj}}\| \approx 0$ then
 return \mathbf{K} , $\mathbb{E}(\alpha(\boldsymbol{\omega}; \mathbf{K}))$, and $\text{Var}(\alpha(\boldsymbol{\omega}; \mathbf{K}))$.
- else
 Increase M_{opt} and repeat starting from step 1, initializing HANSO on the optimal gain value previously found.
- end

Application in vibration control

The proposed method is applied to the case study discussed in the introduction. The method has two stages in the design. Firstly, an acceleration feedback with a distributed-time-delay acceleration [11] is parameterized in order to suppress the undesired oscillations. Secondly, a fixed-order controller optimizing the closed-loop stability of the overall system around a desired set-point is designed with the novel method [1] and it is compared with the one obtained by the deterministic approach [12].

Problem statement

Recall the system shown in Fig. 1 with an active vibration absorber (A) attached to the single-degree-of-freedom primary structure (P). The primary structure has two external inputs. The first f_e is a harmonic force exciting the system with undesirable harmonic oscillations of frequency ω_e . The second input f_u is a controlled input and is meant to provide precise positioning of the system. The force f_a actuating between the primary mass and the absorber has a suppressing effect on the input force f_e .

The dynamic model of the open loop system is in the form

$$\begin{aligned} m_a \ddot{x}_a(t) + c_a \dot{x}_a(t) + k_a x_a(t) - c_a \dot{x}_p(t) - k_a x_p(t) &= f_a(t), \\ m_p \ddot{x}_p(t) + c_a \dot{x}_p(t) + k_a x_p(t) - c_a \dot{x}_a(t) - k_a x_a(t) &= -f_a(t) + f_u(t) + f_e(t). \end{aligned} \quad (9)$$

The physical parameters of the system are m_a , c_a , k_a denoting the mass, damping and the stiffness of the absorber and m_p denotes mass of the primary structure. The parameter of system (9) are given by Table 1.

Table 1: Parameter values for system (9). The values were evaluated in [11, 24].

Parameter	Definition	Mean value	Uncertainty	Units
m_p	Primary mass	1.52	$\pm 20\%$	kg
m_a	Secondary mass	0.223		kg
k_a	Spring stiffness	350		N/m
c_a	Damping ratio of the spring	1.273		kg/s
ω_e	Excitation frequency	13π		rad/s

Consider the feedback in Laplace form as

$$f_a(s) = P(s)x_a(s), \quad (10)$$

where $P(s)$ is a (quasi)polynomial function. Considering zero initial conditions, equations (9) can be expressed as

$$\underbrace{(m_a s^2 + c_a s + k_a)}_{R(s)} x_a(s) + \underbrace{(-c_a s - k_a)}_{Q(s)} x_p(s) = P(s)x_a(s), \quad (11)$$

$$\underbrace{(m_p s^2 + c_a s + k_a)}_{V(s)} x_p(s) + \underbrace{(-c_a s - k_a)}_{Q(s)} x_a(s) = -P(s)x_a(s) + f_u(s) + f_e(s). \quad (12)$$

As mention before, the first task of the control is to design the absorber feedback in a way that the transfer function from f_e to x_p

$$G_{x_p, f_e}(s) = \frac{R(s) - P(s)}{[R(s) - P(s)]V(s) - [Q(s) + P(s)]Q(s)} \quad (13)$$

is zero for the given frequency, *i.e.* the goal is to place a couple of zeros of the numerator of the transfer function (13) as $\hat{s}_{1,2} = \pm j\omega_e$. It is important to notice that $R(s) - P(s)$ is a characteristic function of the active resonator absorber alone. Thus the design of the resonator feedback is independent of the parameters of the primary structure.

Delayed resonator

We consider an absorber control feedback with distributed time delay [11] in the form

$$f_a(t) = \frac{g}{\tau} \int_0^\tau \ddot{x}_a(t - \theta) d\theta, \quad (14)$$

where $\tau > 0$ is the length of the delay, and g is the absorber feedback gain. In this way, function $P(s)$ in (10) is defined as

$$P(s) = \frac{g}{\tau} \left(\frac{1 - e^{s\tau}}{s} \right) s^2. \quad (15)$$

The parameters τ and g are obtained by substituting excitation frequency ω_e into the characteristic equation of the absorber $R(s) - P(s)$, splitting real and imaginary parts, and balancing the magnitudes, see [11] for more details. The resulting terms are

$$\begin{aligned} \tau &= \frac{2}{\omega_e} \left(\operatorname{atan} \left(\frac{c_a \omega_e}{m_a \omega_e^2 - k_a} \right) + 2(l-1)\pi \right), \quad l = 1, 2, \dots \\ g &= \frac{\tau}{2} \left(c_a + \frac{(m_a \omega_e^2 - k_a)^2}{\omega_e^2 c_a} \right), \end{aligned} \quad (16)$$

where l is the branch number denoting a counter associated with phase wrap-around. The branch number is considered as $l = 1$ through the following section, which has a wide stability region, refer to [11] for mode details. Setting the values of Table 1, evaluating (16) gives

$$\tau \approx 5.7355e - 02 \text{ s}, \quad g \approx 4.3017e - 02 \text{ kg}. \quad (17)$$

Controller design

The system (9) with the delayed resonator (14)-(16) can be transformed into a set of first order equation. The system can be explicitly recast as

$$\begin{cases} \dot{x}_a(t) = v_a(t), \\ \dot{x}_p(t) = v_p(t), \\ \dot{v}_a(t) = -\frac{k_a}{m_a}x_a(t) + \frac{k_a}{m_a}x_p(t) + \left(\frac{g}{\tau m_a} - \frac{c_a}{m_a}\right)v_a(t) + \frac{c_a}{m_a}v_p(t) - \frac{g}{\tau m_a}v_a(t - \tau), \\ \dot{v}_p(t) = \frac{k_a}{m_p}x_a(t) - \frac{k_a}{m_p}x_p(t) + \left(-\frac{g}{\tau m_p} + \frac{c_a}{m_p}\right)v_a(t) - \frac{c_a}{m_p}v_p(t) + \frac{g}{\tau m_p}v_a(t - \tau) + \frac{1}{m_p}f_e(t) + \frac{1}{m_p}u(t). \end{cases} \quad (18)$$

Table 1 and equation (17) resume the physical parameter values for the system (18). The uncertainty is contained in the parameter m_p (see Table 1), which we model by $m_p = 1.52 \text{ kg} + \omega$, where the random variable ω is uniformly distributed in the interval $[-0.304, 0.304]$.

The system given by (18) is not exponentially stable for $u \equiv 0$, due to roots at the origin of the complex plane.

We assume that measured outputs of the system are $y = (y_1, y_2)^T$, the position and the speed of the primary cart \mathbf{P} :

$$\begin{cases} y_1(t) = x_p(t), \\ y_2(t) = v_p(t). \end{cases} \quad (19)$$

We now design static and dynamic feedback controllers for the plant (18) with outputs (19). The controller is in the form

$$\begin{cases} \dot{z}_c(t) = A_c z_c(t) + B_c(y(t) - y_{\text{ref}}) & z_c \in \mathbb{R}^{n_c}, \\ u(t) = C_c z_c(t) + D_c(y(t) - y_{\text{ref}}), & u(t) \in \mathbb{R}, \end{cases} \quad (20)$$

where $y_{\text{ref}} = (x_{p,\text{ref}}, 0)^T$ is the reference for the output, with $x_{p,\text{ref}}$ the desired position of the primary mass, A_c , B_c , C_c and D_c are real matrices, and the order of the controller is n_c . In particular, the feedback controller is static if $n_c = 0$, while it is dynamic if $n_c > 0$. In this note we consider a static controller ($n_c = 0$) and a dynamic controller with $n_c = 1$. The goal of optimizing the controller (20) is to find \mathbf{K} minimizing the objective function (4) for different value of the trade-off parameter c .

In order to use the presented Algorithm 1, the system must be rewritten as a delay differential algebraic equations of retarded type. Plant (18), output (19) and controller (20) can be reformulated as a delay differential algebraic equations of retarded type imposing $z = (x_a, x_p, v_a, v_p, y^T, z_c^T, u)^T$:

$$E\dot{z}(t) = A_0(\omega, \mathbf{K})z(t) + A_1(\omega)z(t - \tau) + B(\omega)f_e(t), \quad (21)$$

where \mathbf{K} is the vectorization of the matrices A_c , B_c , C_c and D_c .

Results

The resulting controllers of different orders are listed in Table 2, together with spectral abscissa, mean and variance for the parameters values in Table 1 and equation (17). The controllers obtained by Algorithm 1 with $M_{\text{opt}} = 10^3$ and $M_{\text{post}} = 2 \cdot 10^3$, varying parameter $c = 0, 1, 10, 100$, are compared with the ones evaluated by the deterministic approach [12], *i.e.* minimizing the spectral abscissa for the nominal value $m_p = 1.52 \text{ kg}$. A graphical representation of the values of mean and variance of Table 2 is shown in Fig. 3. By increasing parameter c the mean increases and the variance decreases, which improves the robustness against the parameters uncertainties. On the other hand, the spectral abscissa increases and the system gets slower. Evident improvement can also be seen with the dynamic controller as it has more parameters to tune and hence the optimization has more degrees of freedom.

It is possible to have some insight on the dynamics of the system by looking at an estimates of the probability density functions of the spectral abscissæ for the different controllers, Fig. 4. The deterministic controllers lead to a wider support, with a mode which is usually bigger than the ones obtained with the novel approach. Hence, even though, with the deterministic controller the performance is better at the nominal value, as shown in Table 2, with the novel approach we insure a better convergence rate if the primary mass is affected by an uncertainty. In addition, by increasing the value c we obtain a smaller support insuring a greater insensitivity w.r.t. the parameter m_p .

Moreover, the spectral abscissa for the deterministic dynamic controller admits positive values, revealing the instability of the system for some values of $m_p \in [1.52(1 - 20\%), 1.52(1 + 20\%)] \text{ kg}$. On the other hand, the dynamic controllers obtained by the novel approach lead to a spectral abscissa with support strictly contained in the negative real line, ensuring the stability of the system and the robustness of the method.

Table 2: Numerical value of the spectral abscissa (*i.e.* $\omega = 0$, $m_p = 1.52$ kg), its mean and variance for system (18) with output (19) and with different controllers of the form (19). We consider the mass affected by 20% of uncertainty. To compute the mean and the variance we used $2 \cdot 10^3$ samples. For the deterministic case the spectral abscissa is minimized for the nominal value of the mass, $m_p = 1.52$ kg.

Controller	c	$\alpha(0, \mathbf{K})$	$\mathbb{E}(\alpha(\omega, \mathbf{K}))$	$\text{Var}(\alpha(\omega, \mathbf{K}))$
$n_c = 0$ $k = 2$	det	-7.4454	-4.9881	0.7812
	0	-6.6502	-5.0992	0.8284
	1	-5.8202	-4.7553	0.4451
	10	-4.0842	-3.8331	4.1171e-02
	100	-2.9593	-2.8894	3.6837e-03
$n_c = 1$ $k = 6$	det	-30.6482	-7.0621	99.3767
	0	-9.9397	-10.0416	22.9431
	1	-8.3575	-7.0698	0.8979
	10	-5.5551	-5.5108	2.7537e-02
	100	-4.7510	-4.7474	4.2727e-03

The probability density functions, shown in Fig. 4, are obtained by sampling the spectral abscissa functions as depicted in Fig 5. These latter panes show that the optimal nominal value of the deterministic software [12] corresponds to a non-Lipschitz point of the point $\mathbf{K} \mapsto \alpha(0, \mathbf{K})$, really sensitive to small perturbation of the parameter m_p . On the other hand the spectral abscissa functions with optimal controller obtained by the novel approach varying c , show smoother behavior. A comparison in the time domain is in Fig. 6. The undesired oscillations appear on the primary as the input f_e is exciting the system from $t = 0$ s with amplitude $A = 3$ N. The absorber \mathbf{A} , with its feedback (14)-(17), is attached to the primary structure at time $t = 1$ s while the feedback control (19)-(20) is applied during the whole simulation. As seen, the oscillations affecting the primary mass are suppressed entirely and the primary mass remains stable at the desired position. In time $t = 2.5$ s, the reference position of the primary mass is changed to 10 mm, in formula:

$$\begin{cases} x_{p,ref} = 0 \text{ mm}, & t \in [0, 2.5] \text{ s}, \\ x_{p,ref} = 10 \text{ mm}, & t \in [2.5, 4] \text{ s}. \end{cases} \quad (22)$$

In Fig. 6, the response of the system is as expected from the results in Table 2, the static controllers show slower step response in comparison with the dynamic ones for the nominal value of the primary mass $m_p = 1.52$ kg. By the low variance, the static controllers are insensitive w.r.t. the uncertainty on m_p , even though they present overshoots. We observe performance degradation with dynamic controllers in the deterministic case and for low c . In particular, the system with deterministic dynamic controller is not stable for $m_p < 1.52(1 - 13.65\%)$ kg, computed by Fig. 5, while the dynamic controllers obtained by the novel approach ensure that the system is stable for $m_p \in [1.52(1 - 20\%), 1.52(1 + 20\%)]$ kg. However, in this latter case, the dynamics vary w.r.t. the parameter c : for $c = 0, 1$ we observe performance degradation and the primary structure for $m_p \approx 1.52(1 - 20\%)$ kg oscillates a lot after the reference position is changed, while for $c = 10, 100$ the dynamic is almost insensitive to the change of the primary mass and presents null overshoot.

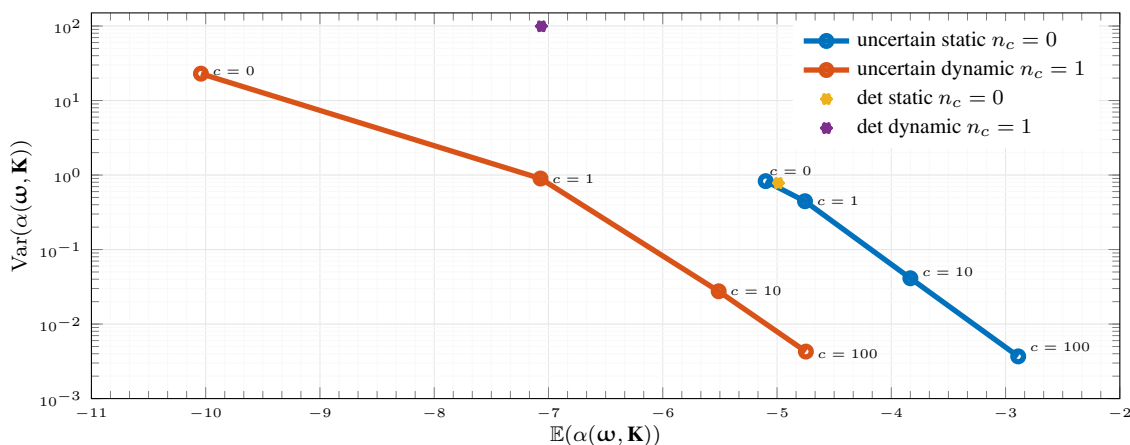


Figure 3: Pareto fronts (*blue and orange lines*) for static and dynamic feedbacks obtained with the novel approach [1] varying the trade off parameter c , and their comparison with the solutions (*yellow and purple dots*) obtained by deterministic method [12].

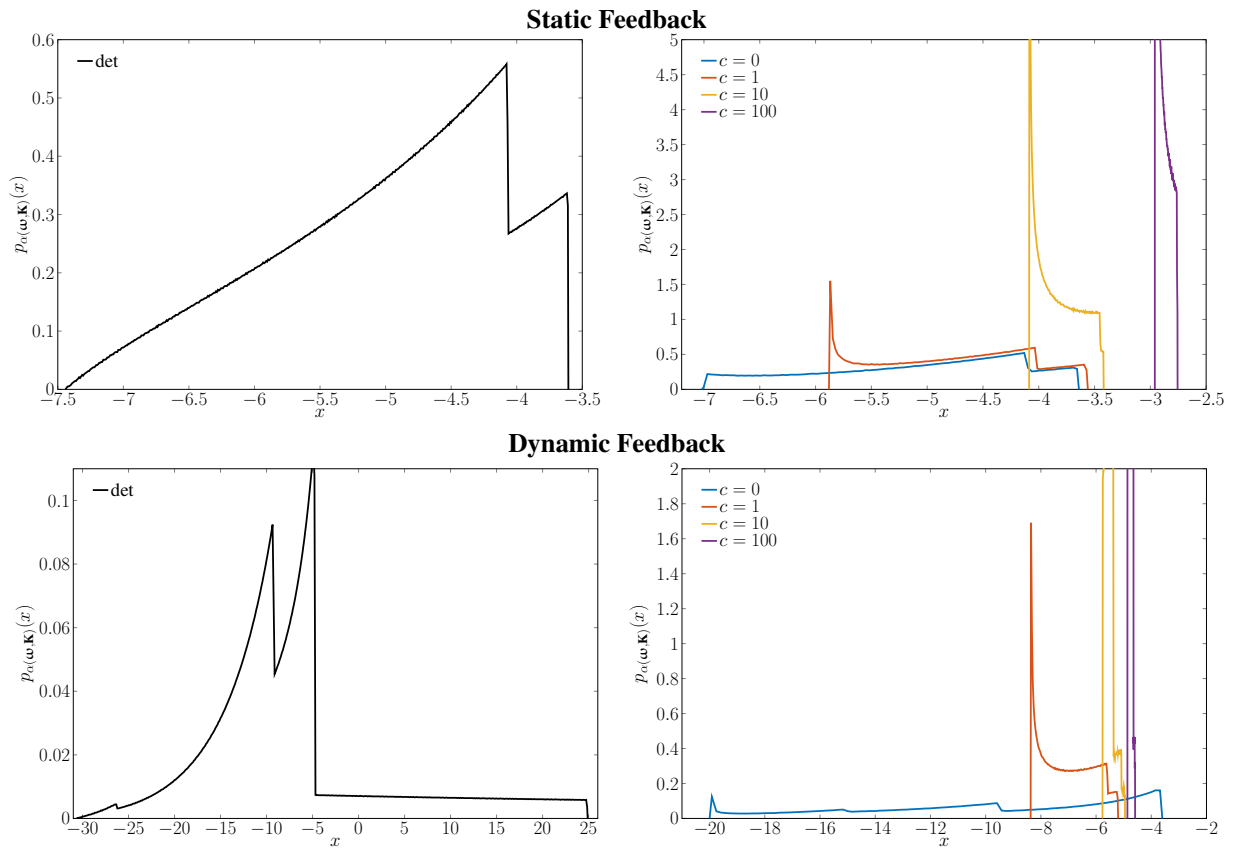


Figure 4: Probability density function of the spectral abscissa for different optimal controllers \mathbf{K} . On the left panes the controllers are obtained by deterministic method [12], on the right panes the controllers are obtained by the novel approach varying c . The probability density functions were estimated by 10^4 samples.

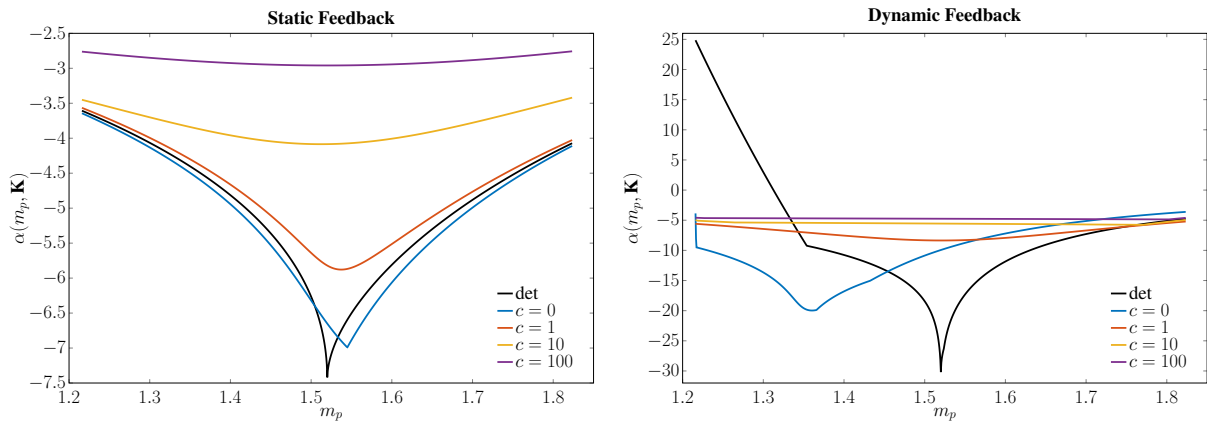


Figure 5: Spectral abscissa functions for different optimal controllers \mathbf{K} varying the uncertain parameter m_p .

Conclusion

The key contribution of this paper is the validation of the novel approach for the design of robust fixed order controller for systems with time delays. The approach considers uncertainty on physical parameters of systems, which results in a closed loop system with increased insensitivity against change of the parameters. We demonstrated the proposed method on the example with an active vibration absorber characterized by distributed delayed feedback. The results are compared with the corresponding deterministic approach [12]. The spectrum of the system was modified in order to stabilize the system and improve robustness against a change of the value of the primary mass, which is not ensured by the deterministic method.

The novel approach permit to obtain different dynamics of stable and robust systems varying the parameter c of objective function (4) and order n_c of the controller. In this way the user, regarding his/her application, may choose the controller based on the different convergence rates and robustness of the resulting system.

In future work we will focus on more complex system and improvement of the optimization speed. We also plan to perform the experimental verification of the proposed scheme.

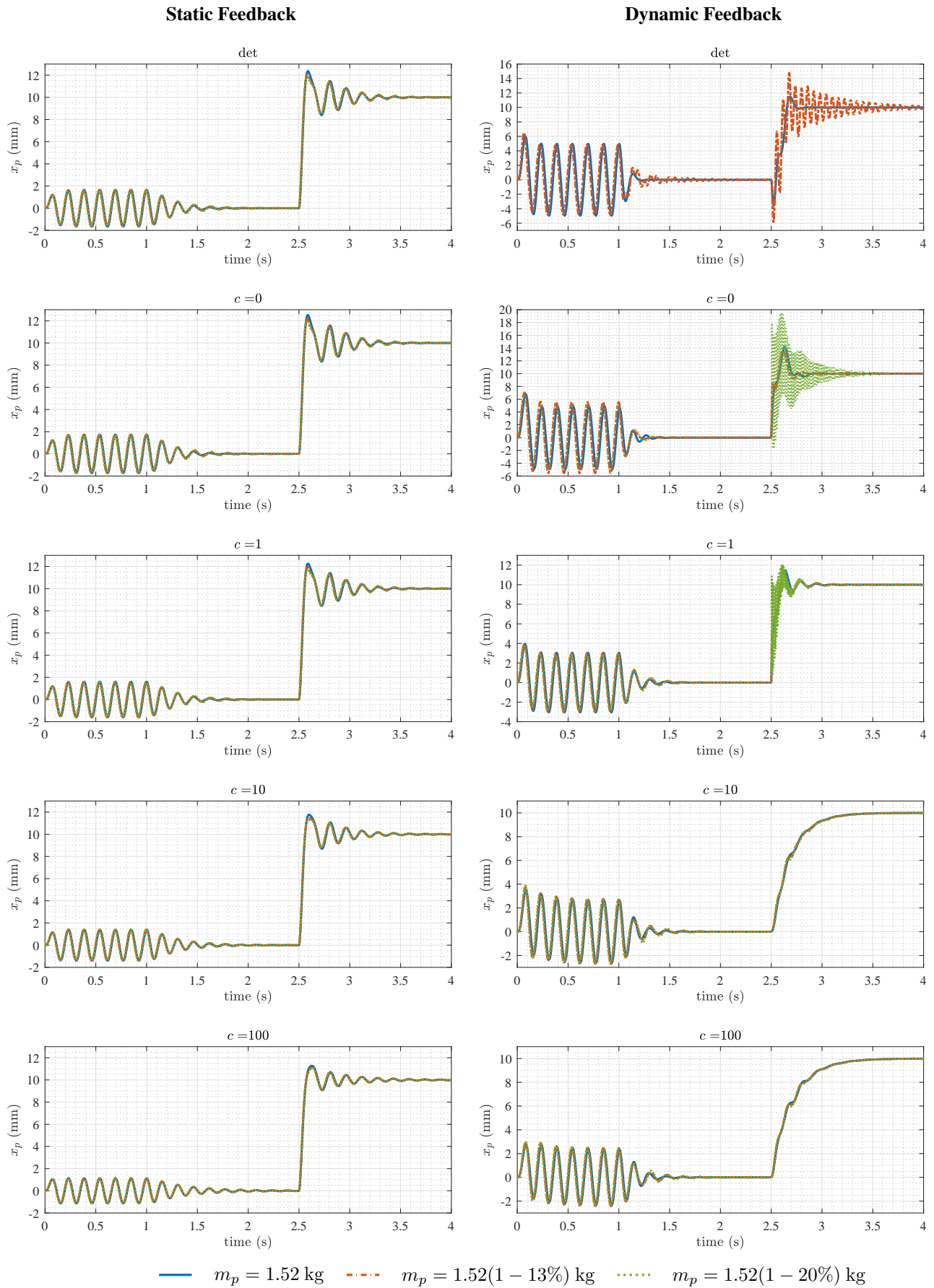


Figure 6: Comparison of dynamics of the position of the primary mass with static and dynamic controllers from Table 2, with different nominal values of the primary mass m_p . In the top-right pane (*deterministic dynamic feedback*), the dynamic for $m_p = 1.52(1 - 20\%)$ kg is not shown, since it is unstable and blows up.

Acknowledgments

This work has been supported by the Program of Interuniversity Attraction Poles of the Belgian Federal Science Policy Office (IAP P6-DYSCO), by OPTEC, the Optimization in Engineering Center of the KU Leuven, by the project G.0712.11N of the Research Foundation-Flanders (FWO - Vlaanderen), by the project UCoCoS, funded by the European Union's Horizon 2020 research and innovation program under the Marie Skłodowska-Curie Grant Agreement No 675080. This work was also supported by the Czech Science Foundation under project No. 17-20943S.

References

1. Fenzi, L. & Michiels, W. Robust stability optimization for linear delay systems in a probabilistic framework. *Linear Algebra and its Applications* **526**, 1–26 (2017).
2. Rivaz, H. & Rohling, R. An active dynamic vibration absorber for a hand-held vibro-elastography probe. *Journal of Vibration and Acoustics* **129**, 101–112 (2007).
3. Alujević, N., Tomac, I. & Gardonio, P. Tuneable vibration absorber using acceleration and displacement feedback. *Journal of Sound and Vibration* **331**, 2713–2728 (2012).
4. Kučera, V., Pilbauer, D., Vyhliđal, T. & Olgac, N. Extended delayed resonators—Design and experimental verification. *Mechatronics* **41**, 29–44 (2017).
5. Olgac, N & Holm-Hansen, B. A novel active vibration absorption technique: delayed resonator. *Journal of Sound and Vibration* **176**, 93–104 (1994).
6. Olgac, N. *Delayed resonators as active dynamic absorbers* US Patent 5431261 A. 1995.
7. Olgac, N. & Holm-Hansen, B. Tunable active vibration absorber: the delayed resonator. *Journal of Dynamic Systems, Measurement, and Control* **117**, 513–519 (1995).
8. Vyhliđal, T., Olgac, N. & Kučera, V. Delayed resonator with acceleration feedback – Complete stability analysis by spectral methods and vibration absorber design. *Journal of Sound and Vibration* **333**, 6781–6795 (2014).
9. Hale, J. K. Strong stabilization of neutral functional differential equations. *IMA Journal of Mathematical Control and Information* **19**, 5–23 (2002).
10. Hale, J. K., M., S. & Lunel, V. *Introduction to Functional Differential Equations* (Springer New York, 2013).
11. Pilbauer, D., Vyhliđal, T. & Olgac, N. Delayed resonator with distributed delay in acceleration feedback: Design and experimental verification. *IEEE/ASME Transactions on Mechatronics* **21**, 2120–2131 (2016).
12. Michiels, W. Spectrum-based stability analysis and stabilisation of systems described by delay differential algebraic equations. *IET Control Theory Applications* **5**, 1829–1842 (2011).
13. Overton, M. L. in *Nonlinear Physical Systems: Spectral Analysis, Stability and Bifurcations* (eds Kirillov, O. N. & Pelinovsky, D. E.) Stability optimization for polynomials and matrices, 351–375 (Wiley-Blackwell, 2014).
14. Michiels, W., Engelborghs, K., Vansevenant, P. & Roose, D. Continuous pole placement for delay equations. *Automatica* **38**, 747–761 (2002).
15. Vanbiervliet, J., Verheyden, K., Michiels, W. & Vandewalle, S. A nonsmooth optimisation approach for the stabilisation of time-delay systems. *ESAIM: COCV* **14**, 478–493 (2007).
16. Michiels, W. & Niculescu, S.-I. *Stability, Control, and Computation for Time-Delay Systems* (Society for Industrial & Applied Mathematics, U.S., 2015).
17. Dick, J., Kuo, F. Y. & Sloan, I. H. High-dimensional integration: The quasi-Monte Carlo way. *Acta Numerica* **22**, 133–288 (2013).
18. Morokoff, W. J. & Caflisch, R. E. Quasi-Monte Carlo Integration. *Journal of Computational Physics* **122**, 218–230 (1995).
19. Caflisch, R. E. Monte Carlo and quasi-Monte Carlo methods. *Acta Numerica* **7**, 1–49 (1988).
20. Breda, D., Maset, S. & Vermiglio, R. Pseudospectral differencing methods for characteristic roots of delay differential equations. *SIAM Journal on Scientific Computing* **27**, 482–495 (2005).
21. Breda, D., Maset, S. & Vermiglio, R. *Stability of Linear Delay Differential Equations* (Springer, New York, 2014).
22. Schreiber, K. *Nonlinear eigenvalue problems: Newton-type methods and nonlinear Rayleigh functionals* PhD thesis (TU Berlin, 2008).
23. Fenzi, L. & Michiels, W. *A MATLAB tool for the Optimization of Uncertain Delay Differential Equations (UD-DAE_optimization)* <http://twr.cs.kuleuven.be/research/software/delay-control/UDDAE_optimization/> (2016).
24. Pilbauer, D., Bušek, J., Kučera, V. & Vyhliđal, T. Laboratory set-up design for testing vibration suppression algorithms with time delays. *Transactions of the VŠB–Technical University of Ostrava, Mechanical Series* **LX** (2014).